BioMetals **14:** 205–222, 2001.

Review

Fluorescence-based biosensing of zinc using carbonic anhydrase

Carol A. Fierke[1] & Richard B. Thompson[2*]
[1]*Departments of Chemistry and Biochemistry, University of Michigan, Ann Arbor, Michigan, USA;* [2]*Department of Biochemistry and Molecular Biology, University of Maryland School of Medicine, Baltimore, Maryland, USA;* [*]*Author for correspondence (Tel: (410) 706-7142; Fax: (410) 706-7122; E-mail: rthompso@umaryland.edu)*

Received 16 January 2001; accepted 27 February 2001

Key words: biosensor, carbonic anhydrase, fluorescence, hippocampus, wavelength ratiometric, zinc

Abstract

Measurement of free zinc levels and imaging of zinc fluxes remains technically difficult due to low levels and the presence of interfering cations such as Mg and Ca. We have developed a series of fluorescent zinc indicators based on the superb sensitivity and selectivity of a protein, human apo-carbonic anhydrase II, for Zn(II). These indicators transduce the level of free zinc as changes in intensity, wavelength ratio, lifetime, and/or anisotropy; the latter three approaches permit quantitative imaging of zinc levels in the microscope. A unique attribute of sensors incorporating biological macromolecules as transducers is their capability for modification by site-directed mutagenesis. Thus we have produced variants of carbonic anhydrase with improved affinity for zinc, altered selectivity, and enhanced binding kinetics, all of which are difficult to modify in small molecule indicators.

Introduction

Zinc is an essential trace element for eukaryotes that is important in diverse biological processes, as discussed in detail in several other articles in this issue of *BioMetals*. In order to better understand the *in vivo* roles of zinc, we have been developing fluorescence-based biosensor approaches for measuring and imaging free zinc in biological specimens, in a manner akin to the methods in use for studying calcium signaling. The measurement of zinc ion flux *in vivo* is complicated by the low concentration of free zinc ions compared to both total zinc and other divalent cations, such as calcium and magnesium. In this article we will describe various protein-based sensing approaches that we have developed to circumvent these difficulties. In particular, we will focus on the development of a carbonic anhydrase-based biosensor, including both the origin of the exquisite metal selectivity in this protein and the various means by which binding of zinc may be transduced as changes in fluorescence.

It is convenient to first define our terms, particularly 'biosensor' and 'transducer'. A sensor (in this

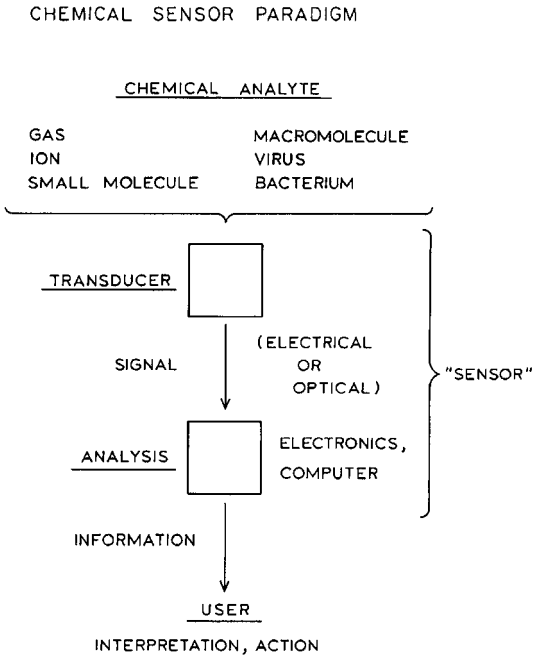

Figure 1. Chemical sensor paradigm

case, a chemical sensor) is a device wherein the presence, amount, or concentration of some chemical analyte interacts with a transducer to produce a signal of some kind (optical and electrical are most common), which can then be converted by some electronic or photonic apparatus into information in a form convenient for interpretation by a human operator (Figure 1) (Thompson & Walt 1994). Although it is not a necessity, in many instances a sensor will also have the capability to measure the analyte continuously for some period, and report the results in real time. While many different approaches are known, a sensor is termed a 'biosensor' if the transducer is a molecule that is biological in origin. In our case the transducer molecule is a variant of human carbonic anhydrase II (CA II), which is found in nature as a metalloenzyme with Zn(II) bound in its active site. The enzymology of CA has been the subject of very thorough study for much of the last century, and the catalytic role of the zinc ion is firmly established (Lindskog *et al.* 1971) . It should be emphasized that the interaction of metal ions with the protein structure is both subtle and elegant, and has been the focus of much inquiry (Christianson 1991; Christianson & Fierke 1996; Hakansson *et al.* 1992; Hunt & Fierke 1997; Lindskog & Nyman 1964). Once the zinc is removed, the *apo*-form of CA binds Zn(II) tightly, specifically, and reversibly in the active site, and from a sensing standpoint CA is not so much an enzyme as a talented ligand.

In view of the numbers of colorimetric and fluorescent indicators described in the literature (Fernandez-Gutierrez & Munoz de la Pena 1985; Haugland 1996; White & Argauer 1970), it is reasonable to wonder why one would develop a biosensor for this purpose. The reasons are primarily selectivity and sensitivity. In many biologically relevant circumstances the data indicate that the concentration of free Zn(II) is quite low, in the range of nanomolar or below based mainly on NMR experiments with fluoro-BAPTA (Benters *et al.* 1997; Denny & Atchison 1994). Clearly any biosensor or indicator would require high affinity to be at least partially saturated and generate an adequate signal at such concentrations. We note that some electrochemical sensors are capable of very high sensitivity (and selectivity) for metal ions such as Cu(II), but their response is necessarily slow at low concentrations, and such electrodes have not yet been described for zinc (Belli & Zirino 1993). Moreover, electrochemical approaches would appear to be ill-suited for imaging. Metallofluorescent indicators are known with fairly high affinity, based on modification of multidentate chelating molecules (Grynkiewicz *et al.* 1985; Kuhn *et al.* 1995; Simons 1993). However, for some applications one might wish for better selectivity and/or sensitivity than these probes currently offer. For instance, Fura-2 (part of a family of fluorescent indicators) is about one hundred-fold more sensitive for Zn(II) than for Ca(II), which suggests its use for measuring Zn(II). However, intracellular calcium levels frequently are high enough to induce a signal (indeed, this is the source of Fura's utility), and extracellular Ca in the millimolar range would naturally saturate the indicator, making its use difficult. Even recently developed metallofluorescent indicators do not match the performance of the CA-based systems. For instance, the indicator ZnAF-1 (Hirano *et al.* 2000) has approximately one thousand-fold worse affinity for zinc (0.78 nM) than wild type CA (0.8 pM) (Hunt *et al.* 1999) (and forty thousand-fold worse than high affinity variants, Table 1). Inasmuch as wild type CA-based fluorescence transducers have demonstrated better than two hundred-fold discrimination between Zn(II) and Cd(II) (Thompson *et al.* 1999) and the affinity of ZnAF-1 for Cd^{2+} remains undisclosed, the latter can hardly be said to be "the first Zn^{2+} sensor molecule that can distinguish Cd^{2+} from Zn^{2+}". Metallofluorescent indicators are discussed by Professor Kimura elsewhere in this issue.

By comparison, *apo*carbonic anhydrase has not only very high affinity, but outstanding selectivity as well (Lindskog & Nyman 1964; McCall & Fierke 2000; Thompson *et al.* 1998a). The X-ray crystal structure of human CA isozyme II (Hakansson *et al.* 1992) reveals that the catalytic zinc ion is coordinated at the bottom of a deep active site cleft by three histidine ligands, H94, H96, and H119, and a solvent molecule in tetrahedral fashion (Figures 2 and 3). At physiological pH, the fourth ligand is provided by hydroxide from solvent. These zinc ligands are fully saturated by hydrogen bonds with other protein residues and are surrounded by a shell of hydrophobic residues. This zinc binding site is retained in numerous isozymes of the alpha class of carbonic anhydrases (Christianson & Fierke 1996) as well as the gamma class (Iverson *et al.* 2000). In contrast, the zinc polyhedron in the beta class of carbonic anhydrases is a $HisCys_2H_2O$ site (Kimber & Pai 2000; Mitsuhashi *et al.* 2000). The dissociation constant of human carbonic anhydrase isozymes I and II for zinc at neutral pH is in the pM range (Hunt & Fierke 1997; Lindskog & Nyman 1964), suggesting the possibility of a very sensitive zinc sensor. Moreover, the metal affinity

Table 1. Variants of carbonic anhydrase.

Variant	K_{zn}, pM	k_{off}, h^{-1}	k_{on}, μM^{-1} sec^{-1}	K_{cu}, pM	K_{Zn}/K_{Cu}	Reference
Wild type	0.8	0.0003	0.1	0.017	50	(Hunt *et al.* 1999; Hunt & Fierke 1997)
H94A	270,000	>140	0.1			(Kiefer & Fierke 1994)
H94C	33,000	0.5	0.004			(Hunt *et al.* 1999; Kiefer & Fierke 1994)
H94D	15,000	0.7	0.01	5	3,000	(Hunt *et al.* 1999; Kiefer & Fierke 1994)
H119D	25,000	10	0.1	80	300	(Hunt *et al.* 1999; Kiefer & Fierke 1994)
H94E	14,000	30	0.6			(Kiefer & Fierke 1994)
H94N	40,000	5	0.03	10	4,000	(Lesburg *et al.* 1997)
H94Q	8,000	20	0.7			(Lesburg *et al.* 1997)
H119Q	70,000	6	0.02	>70,000	< 1	(Lesburg *et al.* 1997)
T199C	1					(Kiefer *et al.* 1993b)
T199E	0.02					(Ippolito *et al.* 1995a)
T199A	60	0.002	0.01			(Kiefer *et al.* 1995)
Q92A	18	0.001	0.02			(Kiefer *et al.* 1995)
E117A	40	1.5	10			(Kiefer *et al.* 1995)
E117Q	4,000	4,680	300			(Huang *et al.* 1996)
Q92A/E117A	160	1.6	3			(Kiefer *et al.* 1995)
F95M/W97V	1.6	2.1	0.4	0.004	400	(Hunt *et al.* 1999; Hunt & Fierke 1997)
F95I/W97S	6	144	6	0.001	6,000	(Hunt *et al.* 1999; Hunt & Fierke 1997)
F93I/F95M	8	0.4	0.01	0.005	1,600	(Hunt *et al.* 1999; Hunt & Fierke 1997)
F93I/F95M/W97V	11	5.8	0.1	0.003	3,700	(Hunt *et al.* 1999; Hunt & Fierke 1997)
F93S/F95L/W97M	29	96	0.9	0.002	14,000	(Hunt *et al.* 1999; Hunt & Fierke 1997)
F93T/F95S/W97V	92	120	0.4	0.0001	900,000	(Hunt *et al.* 1999; Hunt & Fierke 1997)
F93S/F95T/W97M	76	280	1			(Hunt *et al.* 1999; Hunt & Fierke 1997)

of single zinc sites in metalloenzymes is often in this range or higher indicating that these sites should all be saturated even at nM concentrations of zinc.

Carbonic anhydrase has significantly enhanced specificity for zinc, compared to many small molecule metal chelators as discussed above (McCall & Fierke 2000). Nonetheless, other metals do bind; CA binds Cu(II) about an order of magnitude more tightly than Zn(II), Hg(II) with very high affinity, Cd (II), Co(II) and Ni(II) with nanomolar affinity and Mn(II), Mg(II) and Ca(II) with very low affinity, if at all (Lindskog & Nyman 1964; McCall & Fierke 2000; Thompson *et al.* 1998a). In general, the free concentrations of Cu(II) are estimated to be very low in humans (Rae *et al.* 1999) and it seems likely that this is also true for Hg, Cd, Co and Ni, at least in part due to their toxicity, relative scarcity, and the presence of ligands both extracellularly and intracellularly. Consequently, we anticipate (and have found) little interference with Zn sensing using CA-based sensors. Moreover, some of the sensing schemes described below are even more specific for Zn(II) due to the zinc-dependent binding

of the fluorescent aryl sulfonamides, at the active site. In addition, use of a macromolecule transducer, such as CA, confers additional advantages, in that its structure can be subtly altered to 'fine-tune' the selectivity and sensitivity for certain metal ions, as well as the kinetics of binding. Therefore, the tools of genetic engineering can be used to optimize CA as a biosensor using either random mutagenesis and selection techniques ("directed evolution") or structure-based redesign methods (Christianson & Fierke 1996).

Optimization of CA zinc sensor by genetic engineering: Zinc affinity

The main rationale for using carbonic anhydrase as the receptor in a zinc biosensor is that it binds zinc with high affinity and selectivity, as previously described. However, the high zinc affinity of wild-type CA may actually limit the usefulness of a CA-based biosensor. To measure free Zn(II) concentrations in real time, zinc binding must be measured under equilibrium conditions and equilibration must be rapid. Under equilibrium conditions and measuring changes in fluorescence intensity, only zinc concentrations within an order of magnitude of the picomolar Zn(II) dissociation constant of CA (0.1–10 pM) can be accurately measured using a single binding isotherm. While the concentrations of free Zn(II) in biological samples are not yet well-determined in many cases (at least partly due to the lack of a high affinity, selective zinc sensor), the data suggest that the Zn(II) concentration may be higher than 10 pM (Benters *et al.* 1997; Denny & Atchison 1994). Given the uncertainty in the actual Zn(II) concentrations and the possibility of significant fluxes in [Zn(II)], a larger range of detectable zinc concentrations is desirable. One solution to this limitation is to use alternate optical transduction methods that, under certain conditions, can determine zinc concentrations over a larger range (Thompson *et al.* 1998b; Thompson & Patchan 1995a). Alternatively, CA variants with altered zinc affinity could be applied in an array fashion to expand the range of measurable zinc concentrations. To this end, we have successfully used a number of molecular biology techniques, including both structure-based and random mutagenesis, to alter the zinc affinity of carbonic anhydrase by more than 7 orders of magnitude, from 0.02 pM to >1 μM (see below). These mutants, used in an array, could potentially allow quantitation of a wide range of free Zn(II) concentrations ($\sim$2 fM to 10 μM).

We first began altering the zinc affinity of carbonic anhydrase using a structure-based redesign approach. The high resolution structure of CA shows that the single zinc lies at the bottom of a conical cleft where it is coordinated in a tetrahedral fashion by the imidazole side chains of three histidine residues (H94, H96 and H119) and one solvent molecule (Figure 2B) (Eriksson & Jones 1988; Hakansson *et al.* 1992). Studies of both model compounds and proteins suggest that metal affinity and specificity are affected by the geometry of the metal site, including the number and geometric position of the ligands relative to the metal ion and the distances of each ligand from the metal (Alberts & Nadassy 1998; Christianson & Fierke 1996; Glusker 1991; Roe & Pang 1999; Rulisek & Vondrasek 1998). Furthermore, the direct protein ligands of transition metal sites in proteins are typically nested in a hydrogen bond network (Christianson 1991; Christianson & Alexander 1989) and surrounded by a shell of hydrophobic side chains (Yamashita & Wesson 1990). Hence, the entire protein may affect the stability and chemical properties of the protein-metal complex and thus be used to 'tune' the metal affinity. Moreover, these structural features are observable in most metalloenzymes and are likely similarly important for modulating metal affinity, specificity, and reactivity.

The largest alterations in metal affinity in carbonic anhydrase have been obtained by altering the number and chemical nature of the protein side chains that directly coordinate the zinc ion. Removal of one of the ligands, by substitution of histidine with alanine, decreases the zinc affinity by a factor of at least 10^5-fold (Table 1), resulting in a loss of 6–7 kcal/mol of binding energy (Kiefer & Fierke 1994) demonstrating the importance of each of the direct ligands. Surprisingly, replacing the histidine ligands with other residues that could potentially serve as zinc ligands (sulfur of cysteine and the oxygen of glutamate or aspartate) does not enormously increase the binding affinity relative to variants lacking a third protein zinc ligand (Kiefer & Fierke 1994; Kiefer *et al.* 1993a). Variants such as H94C and H94D CA, for example, bind zinc with nanomolar affinity, only approximately 10-fold higher than H94A (Table 1). X-ray crystal structures of these variants (Ippolito and Christianson 1994; Ippolito *et al.* 1995b; Kiefer *et al.* 1993a) reveal that the altered size and shape of the substituted ligand necessitates movement of the surrounding protein structure and/or the zinc ion to maintain tetrahedral geometry. These alterations in the active site structure

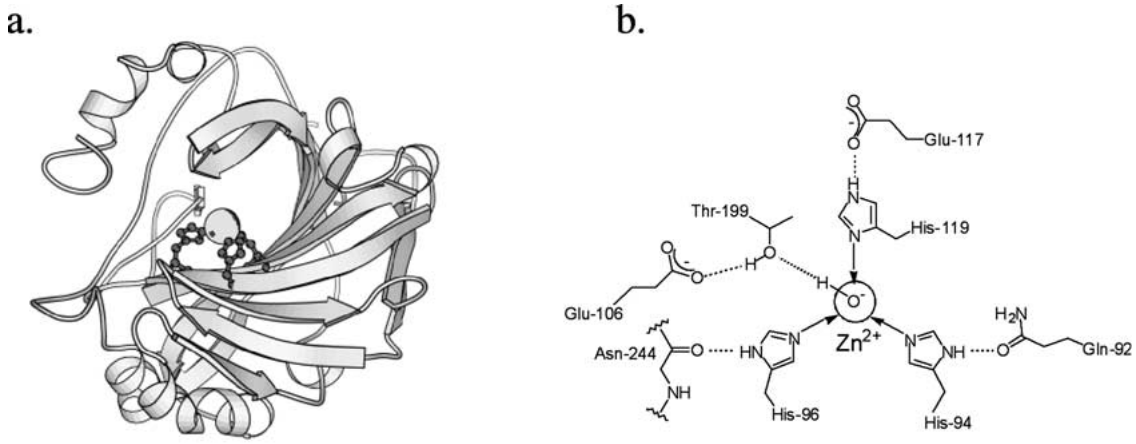

Figure 2. (a) Ribbon diagram of human carbonic anhydrase II; the active site zinc is the sphere coordinated by the three imidazoles. (b) Schematic of active site zinc inner sphere and outer sphere ligands.

are energetically unfavorable, leading to lower binding affinity.

CA metal sites with increased affinity have been created by the addition of a fourth protein ligand to augment the metal polyhedron. Residue T199, which forms a hydrogen bond with the zinc-bound hydroxide of wild type-CA (Figure 2), was substituted with a variety of amino acids capable of directly coordinating zinc, including Cys, Asp, and Glu (Kiefer *et al.* 1993b; Ippolito *et al.* 1995a). Each of these new side chains directly coordinates zinc in tetrahedral geometry, replacing the solvent hydroxide molecule that constitutes the fourth zinc ligand in wild type CA, as demonstrated by high resolution X-ray crystal structure determination (Ippolito *et al.* 1995a; Ippolito & Christianson 1993). The affinity of several of these mutants is comparable to that of wild-type CA (Table 1); in these cases, the favorable energy gained by the additional zinc coordination is virtually offset by the energetically unfavorable movements of the protein. However, the affinity of T199E CA for zinc is greatly enhanced (Ippolito *et al.* 1995a) by addition of this fourth protein ligand, with a K_D of 20 fM, making this the highest affinity zinc site ever engineered.

Additionally, alterations in the hydrogen bond network and hydrophobic shell alter metal affinity. Wild-type CA has four 'second shell' ligands (Figure 2) including hydrogen bonds between the side chains of His 94 and Gln 92, His 119 and Glu 117, and zinc-water and Thr 199. Removal of one of these hydrogen bonds by substitution with alanine decreases metal affinity about 10-fold (Table 1). Furthermore, the decrease in metal affinity is additive

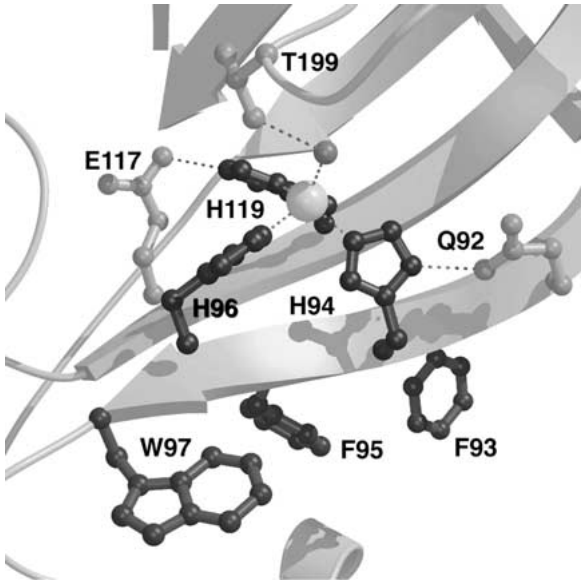

Figure 3. Ribbon diagram of carbonic anhydrase active site showing the zinc ion as a sphere, the inner sphere histidines H94, H96, and H119, and the hydrophobic residues W97, F95, and F93 mutagenized to affect the metal ion binding specificity.

for the Q92A/E117A double mutant, suggesting that the four second-shell hydrogen bonds enhance the protein-zinc affinity by a factor of up to 10^4-fold (Kiefer *et al.* 1995). Calorimetric studies demonstrate that these hydrogen bonds enhance metal affinity by both pre-organizing and desolvating the metal site (DiTusa *et al.* 2001). Alteration of these second-shell ligands allows for subtle changes in the zinc affinity which are essential for creating an array of variants with altered metal affinity.

The shell of hydrophobic side chains surrounding metal binding sites has been proposed to enhance metal affinity by decreasing the mobility of the His ligands or by decreasing the dielectric constant (Yamashita & Wesson 1990). In CA, residues Phe 93, Phe 95, and Trp 97 flank two of the three histidines that coordinate zinc to form a hydrophobic cluster beneath the zinc binding site (Figure 3). To investigate the importance of this hydrophobic shell for determining the metal affinity of CA, we first used cassette mutagenesis to prepare a library of CA variants differing in these three hydrophobic amino acids (Hunt & Fierke 1997). All of these variants were then displayed on filamentous phage as a fusion protein between CA and a minor coat protein (gene 3 protein (g3p)). The phage displaying CA-g3p fusion proteins were then separated on the basis of the zinc affinity of CA using sulfonamide affinity chromatography. Wild-type CA was enriched 20-fold by one round of selection and consensus residues at each position were identified from the enriched variants (I, F, L and M at position 93; I, L and M at position 95; and W and V at position 97). After two rounds of selection, variants that bind to the sulfonamide resin have zinc affinity comparable to that of wild-type CA, indicating that the aromatic residues are not absolutely essential. However, the zinc affinity of mutants containing other substitutions at these positions decreases up to 100-fold (Table 1). Strikingly, the K_{Zn} decreases as the volume of the amino acids at positions 93, 95, and 97 decreases. These experiments demonstrate both that metalloenzyme variants displayed on phage can be selected on the basis of metal affinity and that mutations in the hydrophobic shell can also be used for fine-tuning the zinc affinity of CA.

Zinc specificity

The metal selectivity of WT CA follows the Irving-Williams series (Mn(II)<Co(II)<Ni(II)<Cu(II)> Zn(II)), although the Zn(II) selectivity is increased significantly (several orders of magnitude) compared to most small molecule chelators (Lindskog & Nyman 1964; McCall & Fierke 2000; Thompson *et al.* 1998a). Several features of metal ion binding sites have been hypothesized to alter the transition metal selectivity of chelators. These include: (1) the polarizability of the coordinating atom (Pearson 1966); (2) the relative sizes of the binding site and the metal ion; and (3) the metal ion binding site geometry. Transition metal ions, including Zn(II), Cu(II), and Co(II) are categorized as borderline metals, capable of coordinating O, S, and N with high affinity, but are most often found coordinated to nitrogen (Alberts & Nadassy 1998; Rulisek & Vondrasek 1998). The preferred geometry of metal ions and the optimum ligand distances have been investigated in both model compounds and in proteins (Alberts & Nadassy 1998; Glusker 1991; Roe & Pang 1999; Rulisek & Vondrasek 1998). Zinc is most often observed in tetrahedral geometry in proteins while copper favors square planar and trigonal bipyramidal geometries. In CA, zinc binds with distorted tetrahedral geometry while copper binds with trigonal bipyramidal geometry (Hakansson *et al.* 1992, 1994) .

To investigate whether the metal selectivity is tuned by the geometry of the ligands in the metal binding site, we measured the relative affinity and selectivity for various transition metals of mutants of residues Phe93, Phe95 and Trp97 which are located on the same β-strand as two of the histidine ligands (Figure 3) (Cox *et al.* 2000; Hunt *et al.* 1999). Although the zinc and cobalt affinity of these variants decreases as the hydrophobicity of the substituted side chains decreases (Hunt & Fierke 1997), the copper affinity *increases*, resulting in a significant net enhancement in the selectivity of the enzyme for copper (Hunt *et al.* 1999). These data suggest that the hydrophobic shell does not enhance zinc affinity mainly by altering the dielectric constant of the metal binding site. X-ray crystal structures of metal-bound F93I/F95M/W97V and F93S/F95L/W97M CAs (Cox *et al.* 2000) reveal that the coordination geometry of the zinc-bound and copper-bound enzymes remain tetrahedral or trigonal bipyramidal, respectively, as observed in WT CA. However, a conformational change of the direct metal ligand H94 as well as the indirect ligand Q92 occurs in the apo-form of the mutants, thereby eliminating the preorientation of the histidine ligands into a tetrahedral geometry, as observed in the apo-WT enzyme (Hakansson *et al.* 1992). This increased flexibility enhances formation of 5-coordinate trigonal bipyramidal metal coordination geometry relative to 4-coordinate tetrahedral geometry, which in turn increases Cu(II) affinity and decreases Zn(II) affinity. These data demonstrate that aromatic core residues serve mainly a foundational role, as anchors that help to preorient direct and second-shell ligands to optimize the zinc binding geometry and to destabilize alternative geometries. Therefore, the zinc/copper selectivity in CA, and likely other proteins as well, is tuned

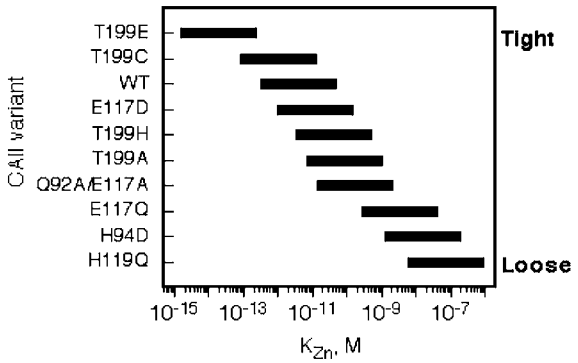

Figure 4. Zinc affinities of variants. Variants are ranked with the highest affinities at the top to lowest at the bottom; the bars give the range of free zinc ion concentration that can be accurately measured by a particular variant.

by stabilizing the preferred tetrahedral geometry of zinc and destabilizing the trigonal bipyramidal copper geometry (Cox *et al.* 2000; Hunt *et al.* 1999).

In addition to enhancing our understanding of zinc affinity and selectivity in proteins, we have prepared a series of variants of CA whose zinc affinity ranges over seven orders of magnitude (Figure 4), and with a range of selectivity as well. The broad range of affinities is of use because an appropriate variant can be chosen which responds well for any given free zinc level from one femtomolar to one micromolar. By comparison, known metallofluorescent zinc indicators respond down to below one nanomolar, but quantitation at levels below this remains troublesome.

Zinc equilibration

A second factor limiting the utility of wild-type CA in a zinc sensor is the extremely slow zinc dissociation rate constant. The $t_{1/2}$ for this dissociation is estimated to be on the order of months (Hunt & Fierke 1997; Lindskog & Nyman 1964), virtually limiting the sensor to a single use rather than continuous, real-time monitoring. In CA, zinc equilibration is limited by both the high zinc affinity (pM) and the slow zinc association rate constant of 10^5 M^{-1} s^{-1} (Henkens & Sturtevant 1968; Kiefer & Fierke 1994), 10^3-fold slower than the diffusion-controlled limit of 10^7–10^8 M^{-1} s^{-1} (Eigen & Hammes 1963). Since the rate constant for zinc equilibration can be approximated by k_{on} [L] + k_{off} and since $K_D = k_{off}/k_{on}$, the observed zinc equilibration rate can be enhanced by increasing k_{on} and/or k_{off}. In mutants with decreased zinc affinity (as described above), the zinc dissociation rate constants often increase (Hunt & Fierke 1997; Kiefer & Fierke 1994; Kiefer *et al.* 1995), roughly paralleling the K_D (Table 1). These mutants therefore further enhance the utility of CA-based zinc sensors.

In some cases, however, the zinc dissociation rate constant increases significantly more than the metal affinity decreases, suggesting that the zinc association rate constant increases significantly (Table 1). In particular, substitution of Glu-117, the hydrogen bond partner of the direct ligand His-119 (Figure 2), with either alanine or aspartate causes the K_D to increase 3- to 10-fold while the dissociation rate constant increases 30- to 70-fold (Kiefer *et al.* 1995; Lesburg & Christianson 1995). Therefore, the calculated zinc association rate constant increases significantly, to $\sim 10^7$ M^{-1} s^{-1} and the half-time for zinc dissociation decreases to about 30 minutes. Additionally, substitution of Glu-117 with Gln causes further increases in K_D and k_{off} (Table 1) (Lesburg *et al.* 1997). In this variant the calculated zinc association rate constant of 3×10^8 M^{-1} s^{-1} is at or near the diffusion-controlled limit and the half-time for zinc dissociation, 0.6 s^{-1}, is certainly fast enough for most biosensor applications. These data indicate that hydrogen bonds between the direct zinc ligands and indirect hydrogen bond acceptors are a primary factor controlling the slow association and dissociation of zinc. These hydrogen bonds may affect zinc equilibration by pre-orienting the metal binding site to reduce conformational energy.

These detailed structure-function studies provide an understanding of the mechanism of metal binding in CA and allow the prediction of additional amino acid substitutions that will affect the properties of the metal binding site. The current CA variants with altered metal affinity, specificity and equilibration kinetics are extremely useful in developing real-time metal ion biosensors. Our demonstrated ability to tune both the metal affinity and metal equilibration kinetics by subtly altering the packing of the zinc binding site has no counterpart in small molecule metallochromic or metallofluorescent indicators, nor in ionophores for electrochemical methods, illustrating the versatility of biological receptors.

Transducing zinc binding as a fluorescence signal

Although *apo*-CA is a very selective, high affinity ligand for Zn(II), it is also necessary that zinc binding creates a signal which can be readily observed and

measured. For speed, simplicity, and to avoid the need to consume reagents we do not find transduction employing the enzyme activity itself to be attractive. For use in observing tissues and cells it is desirable that it be an optical signal, preferably fluorescence owing to its sensitivity, flexibility, and the widespread availability of fluorescence microscopes. For a continuous monitor (as opposed to a single determination) the reversible binding of the zinc ion should result in a reversible change in the fluorescence. Thus we would like to arrange matters such that binding of zinc to *apo*-CA results in a change in fluorescence, which we can readily measure, and that dissociation of the metal from the protein reverses that change. Of course, the fractional saturation of the binding site is controlled by the law of mass action, and in particular the concentration (more properly, the activity) of the metal ion.

The vast majority of metallofluorescent indicators transduce metal ion binding as changes in fluorescence intensity: e.g., in most cases interaction with the metal ion results in a change in quantum yield of the fluorophore, leading to a change in the intensity of fluorescence. Attempting to relate a measured fluorescence intensity to an analyte concentration is very prone to artifact, and is seldom done either clinically or in research. Recognizing this problem in attempting to measure Ca(II) concentrations with indicators such as calcein, workers turned to the so-called wavelength-ratiometric probes developed by Roger Tsien and his colleagues. Among these are Fura-2, Indo-1, and a host of successors (Grynkiewicz *et al.* 1985; Haugland 1996). These probes exhibit a shift in excitation and/or emission spectra upon binding the metal, and consequently the ratio of intensities at the two peaks is proportional to the ratio of indicator with metal bound and free. Measuring a ratio of fluorescence intensities instead of a simple intensity eliminates many of the artifacts present in such measurements, and makes calibration more straightforward. Transducing the binding of the metal as a change in fluorescence anisotropy (polarization) confers similar advantages (Thompson *et al.* 1998a; Weber 1956), because the anisotropy can also be measured as a ratio of two intensities. Fluorescence anisotropy microscopy has been known for some time (Dix & Verkman 1990; Fushimi *et al.* 1990). Finally, one can also transduce the binding of the metal as a change in fluorescence lifetime, which similarly avoids the artifacts associated with simple intensity measurements. Moreover, lifetime measurements (as with anisotropy measurements) can under certain conditions exhibit a much broader dynamic range of analyte concentration than is achievable with either simple intensity or intensity ratio measurements (Szmacinski & Lakowicz 1993; Thompson *et al.* 1998b; Thompson & Patchan 1995a). However, lifetime measurements remain complex and relatively expensive, despite advances in instrumentation for their measurement and imaging.

Finally, lifetime measurements are very well suited to configurations of the biosensor wherein the CA is immobilized on quartz, glass, or some other suitable substrate (Clark *et al.* 1999) which is immersed into a solution (such as the cytoplasm of a cell), permitting the Zn level to be measured continuously. A particularly useful example is immobilization on the distal tip of a fiber optic, which can then be inserted into the bloodstream or interstitial spaces of an experimental animal to measure the analyte *in situ* (Thompson 1991). This is a potentially powerful research and diagnostic tool which we hope to exploit for zinc studies.

Zinc sensing using fluorescent aryl sulfonamides and CA

The first approach to fluorometrically determining zinc using carbonic anhydrase built on the pioneering work of Chen & Kernohan (1967). They discovered that dansylamide, one of the class of aryl sulfonamide inhibitors of the enzyme, exhibited dramatic changes in its fluorescence upon binding to *holo*carbonic anhydrase. Aryl sulfonamides had long been known to inhibit the enzyme (Maren 1977), and due to their therapeutic importance in treating glaucoma, hundreds of such compounds had been identified. It was well understood that the inhibition was based upon the active site zinc promoting the ionization of the (weakly acidic) sulfonamide when it is bound, in a manner precisely analogous to the water ordinarily bound as a fourth ligand. The fluorescence of dansyl is well known to be environment-sensitive, and consequently its emission is substantially blue shifted and enhanced upon binding to the enzyme (Figure 5). Thompson and Jones (1993) showed in the absence of the metal that dansylamide's affinity was much reduced, and consequently the fluorescence of dansylamide could be used as an indicator of zinc's presence in the active site. Since the occupancy of the zinc binding site is controlled by the free zinc ion concentration through the law of mass action, one could relate the change in

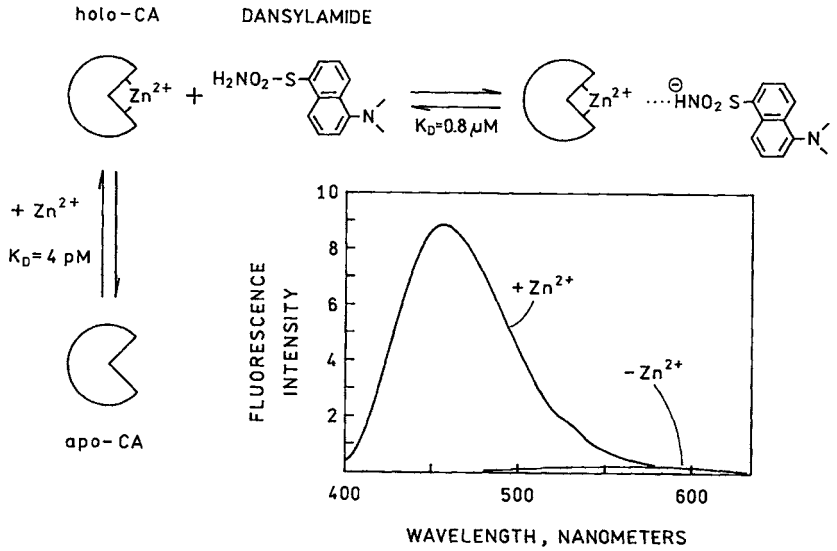

Figure 5. Dansylamide sensing scheme. Free dansylamide emits weak fluorescence (*inset*) in the presence of apo-CA, but when Zn(II) binds to CA, dansylamide binds to holo-CA, emitting strong blue fluorescence.

fluorescence observed to the concentration of zinc. By itself, dansylamide has essentially no affinity for the metal.

In fact, dansylamide's fluorescence changes in several ways upon binding to the protein, each of which may be used to determine zinc concentration. Perhaps most important is the dramatic 100+ nm blue shift and seven-fold increase in quantum yield, because it permits a ratiometric measurement of intensities at emission wavelengths corresponding to the free (560 nm) and bound (450 nm) forms of dansylamide. While this approach enjoys some of the well-known advantages of the ratiometric measurements it should be remembered that it is not entirely insensitive to the concentrations of dansylamide and apoprotein in use. The large change in fluorescence lifetime of dansylamide may also be used in the same way to determine zinc. Although measuring changes in fluorescence lifetime requires more sophisticated instrumentation than measuring intensities, this approach has particular advantages for measurements through fiber optics (Thompson 1991; Thompson 1993). Moreover, the instrumentation is becoming simpler and cheaper (Levy *et al.* 1997; Lippitsch *et al.* 1988; Thompson *et al.* 1992). Finally, under certain circumstances lifetime measurements can exhibit an enhanced dynamic range (Szmacinski & Lakowicz 1993; Thompson & Patchan 1995a); we subsequently showed anisotropy measurements offer the same advantage (Thompson *et al.* 1998b).

Dansylamide suffers from two key drawbacks: first, its extinction coefficient is rather low (ε_{330} = 3300 M^{-1} cm^{-1}), limiting sensitivity. Second, the short wavelength UV necessary for excitation is a problem owing to the expensive microscope optics required, the inconvenience of exciting at these wavelengths, and the high autofluorescence background observed in natural specimens. Clearly it was desirable to have a longer wavelength probe; consequently, we developed ABD-N and ABD-M (Figure 6). These compounds are excitable in the visible and have 2–3 fold larger extinction coefficients than dansylamide, but also exhibit shifts in excitation and emission upon binding to holo-CA, as well as changes in quantum yield, lifetime, and anisotropy (Table 2) (Thompson *et al.* 2000a, 1998b). ABD-N is the more useful due to its higher quantum yield when bound compared with ABD-M. ABD-N can be used to quantitate zinc by changes in intensity, lifetime, anisotropy, or wavelength ratio; the last is illustrated in Figure 7 (Thompson *et al.* 2000a). Both molecules are adequately water-soluble.

In looking for additional fluorescent aryl sulfonamides which might be useful for this approach, we found two others which are noteworthy. The first is Dapoxyl sulfonamide (Figure 6), which in a sense is complementary to ABD-N in that it exhibits a very

Table 2. Aryl sulfonamides used in zinc sensing.

Probe	Free/Bound	λ_{exc}, nm	λ_{em}, nm	QY, relative	$< \tau >$, nsec	K_D, μM	log ε	aniso	ratio	λ_1/λ_2	References
DNSA	Free	330	560	0.08	3		3.52		0.039	450/560	(Chen & Kernohan 1967; Thompson & Jones 1993)
	Bound		450	0.55	22.1	0.8			1.6		
ABD-N	Free	435	602	0.086	0.34		3.94	0.09	3	560/680	(Thompson *et al.* 2000a)
	Bound	420	558	1.0	4.98	0.9		0.23	7.5		
ABD-M	Free	390	528	0.33	0.8		3.9	0.03			(Thompson *et al.* 1998b)
	Bound	380	492	1.0	1.53	0.3		0.32			
Azosulfamide	Free	501				0.01	4.5				(Thompson & Patchan 1995b)
	Bound										
Dapoxyl sulfonamide	Free	365	615	0.01	0.22		4.3		3	535/685	(Thompson *et al.* 2000b)
	Bound		535	1.00	3.60	0.13			38		
BTCS	Free	466	504	0.88	2.53		4.56	0.05			(Thompson *et al.* 2000b)
	Bound			1.00	2.71			0.25			
Elbaum's	Free	495	505	1.0	4.0		4.9	0.01			(Elbaum *et al.* 1996)
	Bound			0.96		0.002		0.10			

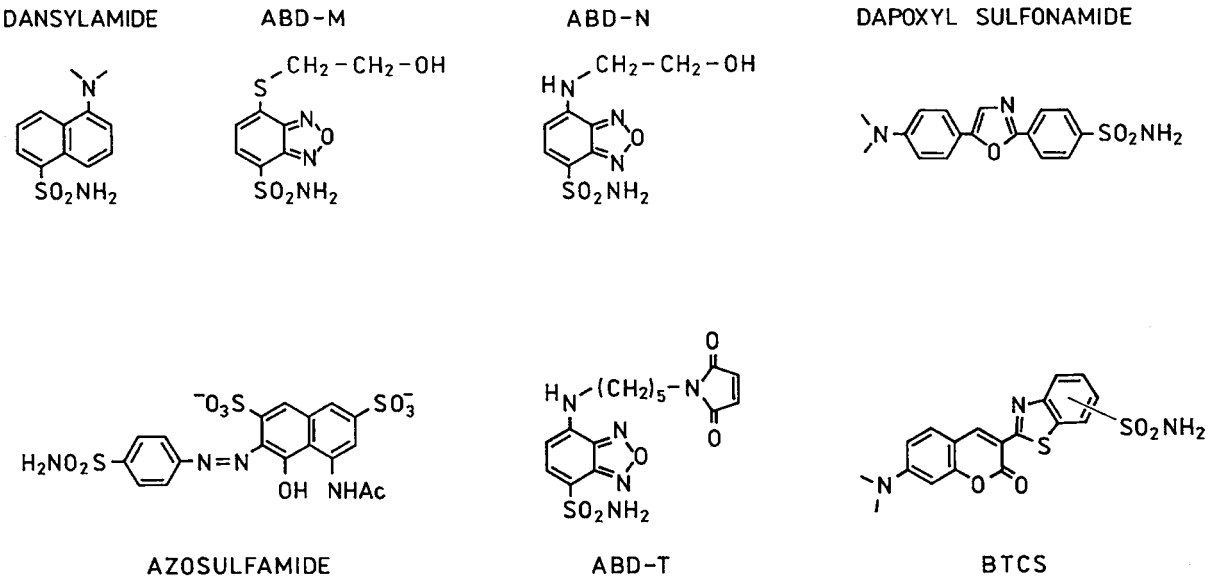

Figure 6. Aryl sulfonamides which bind to carbonic anhydrase.

large fluorescence enhancement upon binding to holo-CA, together with a large blue shift in its fluorescence. However, it has twice as large an extinction coefficient as ABD-N (Table 2). Unlike ABD-N, however, it penetrates cells readily, and stains membrane bilayers. The fluorescence of the bilayer-bound form differs from the CA-bound form, but not dramatically so (Thompson *et al.* 2000b), making intracellular zinc measurements problematic at the present time. It has a significant two-photon excitation cross section, but is not a good anisotropy probe. By comparison, the benzothiazolyl coumarin sulfonamide BTCS (Figure 6) exhibits little change in lifetime or quantum yield upon binding to CA, which makes it an excellent anisotropy probe (Thompson *et al.* 2000b). Spectroscopically, it is similar to the fluorescein moiety in our original anisotropy probe (Elbaum *et al.* 1996), and has a high quantum yield and extinction coefficient.

Fluorescence energy transfer-based zinc biosensing

The environment-sensitive fluorophores most useful in the aryl sulfonamide approach depicted above are in general poor absorbers which often must be excited at relatively short wavelengths. Partly to avoid this problem a more flexible approach was sought. Among the hundreds of aryl sulfonamide inhibitors known, several are colored but otherwise nonfluorescent, and therefore useless in the approach outlined above. However, the propensity of these colored aryl sulfonamides to bind to the holoprotein at the active site when zinc was present (and not to bind in its absence) suggested a somewhat different approach. In particular, it was straightforward to fluorescently label the protein with a covalent derivative, chosen for overlap of its emission with the absorbance of the colored aryl sulfonamide. If the colored sulfonamide binds at the active site it is perforce brought within 25 Å of the label, which thus partly quenches the fluorescence of the label due to Förster resonance energy transfer (Figure 8). In the absence of zinc the sulfonamide is free to diffuse away, so no energy transfer occurs and there is no diminution of the label's emission. Importantly, the lifetime of the label declines commensurately with the intensity, permitting the zinc's quantitation by time-resolved fluorescence measurements, which are more robust than intensity measurements. The response of the system can be optimized by careful selection of the label and colored arylsulfonamide based on their known spectral properties. Use of site-directed CA mutants permitted the label to be positioned in a defined and predetermined fashion to optimize the response (Thompson *et al.* 1996a; Thompson & Patchan 1995b).

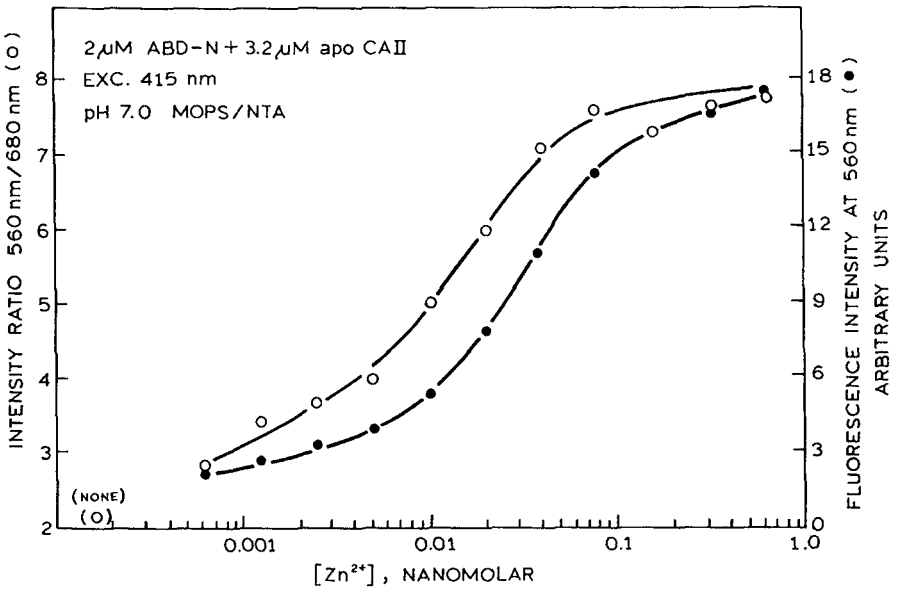

Figure 7. Fluorescence emission intensity at 560 nm (filled circles) and emission intensity ratio at 560 nm/680 nm (open circles) for 3.2 μM apo CA + 2.0 μM ABD-N; excitation at 415 nm.

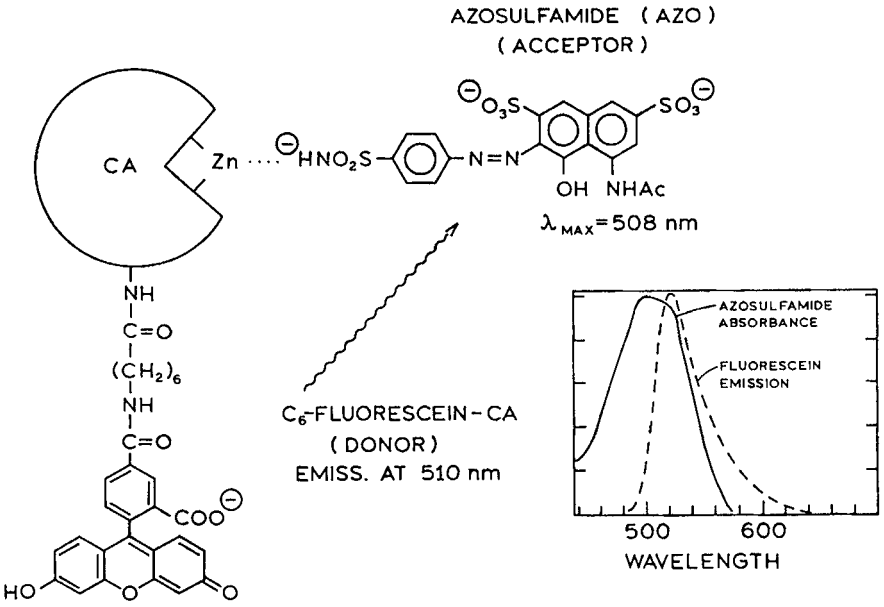

Figure 8. Fluorescence energy transfer zinc sensing approach. In the presence of zinc, azosulfamide binds to the holo-CA and accepts energy from the donor, quenching it; in the absence of zinc, azosulfamide does not bind to the apo-CA and no energy transfer occurs, maintaining the fluorescence intensity and lifetime of the donor. The *inset* shows the spectral overlap of the fluorescein donor emission (dashed line) with the azosulfamide absorbance (solid line).

Zinc sensing using fluorescent-labeled CA

The use of a separate, small molecule such as the aryl sulfonamides described above together with the protein CA has certain drawbacks. First, while CA is a macromolecule that does not ordinarily penetrate lipid bilayers, the aryl sulfonamides are small molecules which can (in some cases), so the two may partition differently in cells. Also, in the case of Dapoxyl sulfonamide the fluorophore binds to bilayers, emitting fluorescence which potentially interferes with that from the fluorophore bound to holo-CA. At some fundamental level, one would like the fluorescent moiety to go anywhere the protein went; e.g., that they be covalently attached. This is termed a 'reagentless' transducer, in that no separate reagent is necessary.

While we have described several fluorescently-labeled CA variants which exhibit changes in fluorescence upon binding metal ions such as Cu(II), Co(II), and Ni(II) (Thompson *et al.* 1996b, 1998a, 1999), it has been somewhat more difficult to design transducers for Zn(II). This is because (unlike the other metals) Zn(II) is not a very good quencher of fluorescence owing to its low atomic number, diamagnetic character, and difficulty of reduction. By comparison ions such as Cu(II), Ni(II), Hg(II), or Co(II) are typically good quenchers because they are paramagnetic, of high atomic number, and/or readily reduced or oxidized. Thus two new approaches were followed with a view to having the presence of zinc in the CA binding site alter the fluorescence of a nearby fluorophore. The rationale for the first was that an environment-sensitive fluorophore in the immediate vicinity of the binding site might well detect a difference between when the binding site was occupied with the zinc ion and when it was unoccupied. The fluorophore-variant combination that showed the greatest differences in fluorescence was N67C-ABD, but these changes (see below) were not attributable to the changes in solvent polarity that manifest themselves as shifts in excitation and emission, such as occur with dansylamide or ABD-N. We also designed another covalently attachable derivative of the ABD fluorophore with an n-hexyl tether (ABD-T) (Thompson *et al.* 1998a), with the objective of attaching it to the protein through a long, flexible link so as to permit it to bind as a fourth ligand to the active site zinc, and exhibit the overt fluorescence changes typical of ABD-N and dansylamide. While this did not occur, the response was still useful, especially with regard to anisotropy and lifetime (see below).

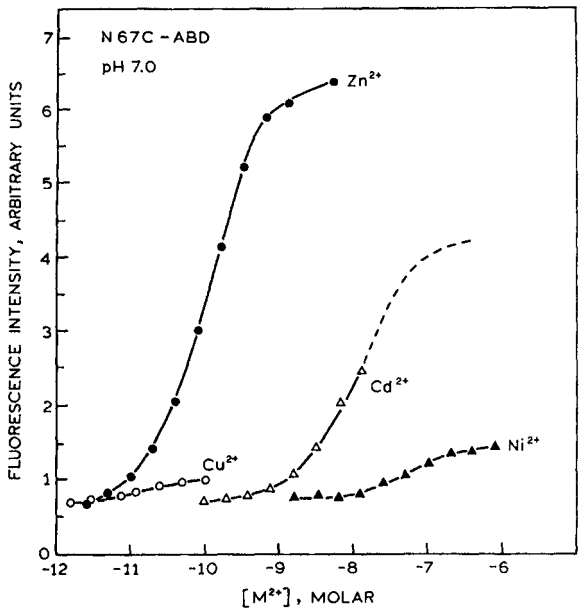

Figure 9. Fluorescence intensity of N67C-ABD as a function of Zn (filled circles), Cu(II) (open circles), Cd(II) (open triangles), and Ni(II) (filled triangles).

N67C-ABD did not show the response expected if there were a change in the polarity of its environment, in that there is little or no shift in the emission or excitation upon zinc binding (Thompson *et al.* 1999). However, there is a substantial increase in intensity and lifetime upon binding zinc. More unusual are the lesser increases in intensity and lifetime upon binding other metal ions (Figure 9). This may be rationalized by considering the fluorescent aryl sulfonamide derivative of β-mercaptoethanol, ABD-M (Table 2). ABD-M shows a short lifetime and modest quantum yield free in solution like its amine cousin, ABD-N; however, upon binding to the holoenzyme it exhibits a more modest increase in quantum yield and lifetime than ABD-N, which makes it a better anisotropy probe. In view of the longer average lifetime and higher apparent quantum yield of ABD-N, it is evident that ABD-M is still fairly well quenched even when bound. It may be that binding offers a degree of protection from quenching by, for instance, water. In the case of N67C-ABD the presence of zinc may limit the accessibility of the fluorophore to water, effectively 'dequenching' it. The other metal ions have the same effect, only they themselves (notably copper and cobalt) also quench the fluorophore by other mechanisms, making the intensity and lifetime enhancements less in their cases. Although it produces

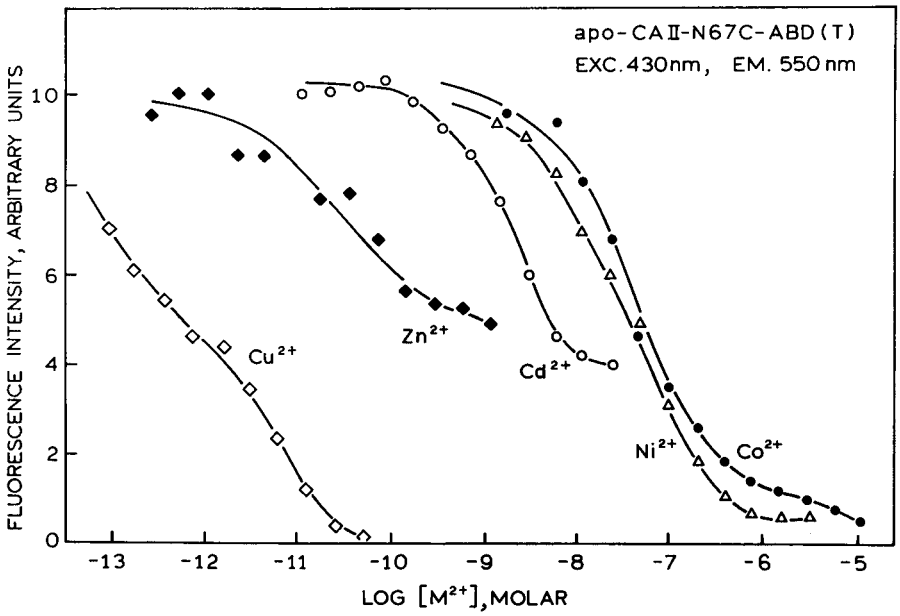

Figure 10. Fluorescence intensity of N67C-ABD-T as a function of Cu(II) (open diamonds), Zn(II) (filled diamonds), Cd(II) (open circles), Ni(II) (triangles), or Co(II) (filled circles) concentration.

a fairly good fluorescence enhancement, one cannot increase the signal by looking selectively at the bound form's emission because the shift is negligible.

The tethered form of ABD, ABD-T, also did not respond as expected, in that when coupled to the introduced thiol at position 67 (N67C) it exhibited no shift in emission or excitation upon zinc binding, effectively ruling out interaction of the sulfonamide moiety with the zinc. In its case zinc quenches the fluorescence (as do the other metals), resulting in reduced intensity (Figure 10) and lifetime, with increased anisotropy (Figure 11). The responses are quite satisfactory, but for intensity imaging purposes the decline in intensity is less desirable than an increase.

Application to studies of brain zinc

Zinc is an ion of substantial biological interest in many respects, as is discussed elsewhere in this issue. One important question is the role of the weakly bound zinc found in axonal boutons in the cortex, especially the hippocampus. Understanding the biological and pathological role(s) of zinc in the brain had been hampered by the difficulty of measuring zinc levels even extracellularly, owing to the high levels of interfering calcium and magnesium, and the transient localized nature of the release upon stimulation.

Recently, ABD-N has been used together with apo-CA to image zinc release from rat hippocampus in organotypic cell cultures (Thompson *et al.* 2000a) and classical slice preparations. For these experiments the apo-CA and ABD-N are incorporated into the artificial cerebrospinal fluid (ACSF) bathing the neural tissue. Because of the high affinity of CA for zinc, the ACSF must be specially prepared to avoid contamination. In particular, the ACSF (minus Ca and Mg) is passed over a chelating resin to remove zinc and other potential interferents, whereupon high purity Ca and Mg salts (electronic or similar grade) are added; ordinary reagent grade salts have unacceptable levels (several parts per million) of metallic impurities. Release is stimulated either electrically, with a brief pulse train, or by other insults (Frederickson *et al.* 2000). The concentration of free zinc may be quantitated ratiometrically (Figure 7) and the kinetics of zinc release quantitated through the microscope (Figure 12) (Suh *et al.*, submitted). We observed these slow release kinetics in our initial experiments (Thompson *et al.* 2000a), but believed that the apparent slow release (over tens of seconds) was due to the slow association rate constant of the wild type enzyme used (Thompson *et al.* 2000c), and that only nanomolar zinc concentrations were present. In fact micromolar levels are present, as may be seen in Figure 12, which also underscores the importance of quantitative methods.

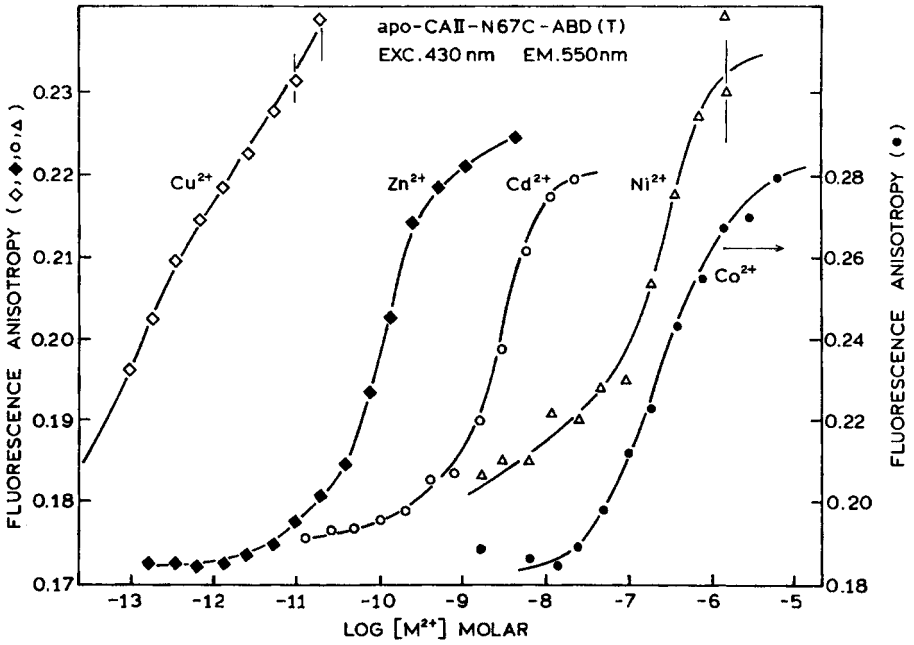

Figure 11. Fluorescence anisotropy of N67C-ABD-T as a function of Cu(II) (open diamonds), Zn(II) (filled diamonds), Cd(II) (open circles), Ni(II) (open circles), or Co(II) (filled circles) concentrations.

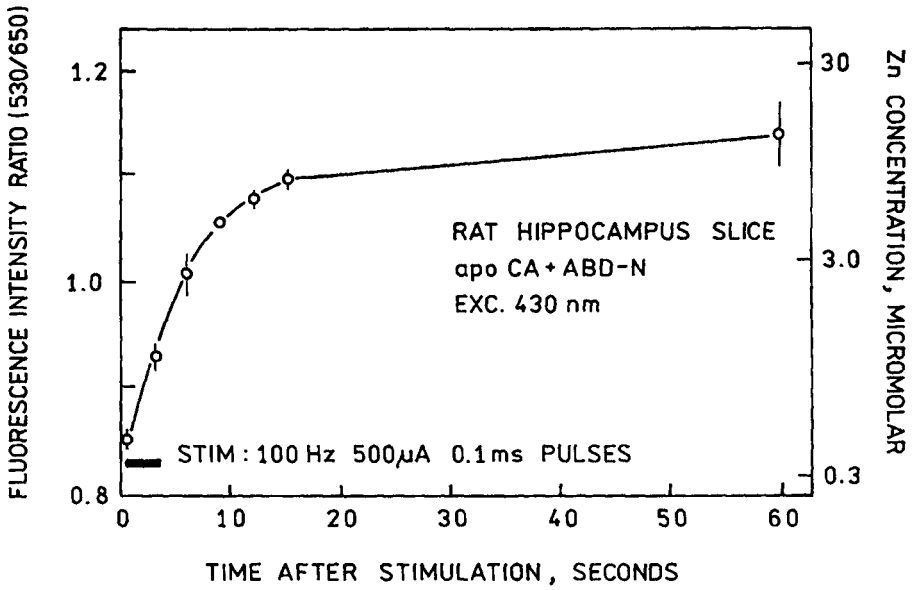

Figure 12. Kinetics of Zn(II) release from rat hippocampal slice preparation following electrical stimulation at the dentate gyrus (unpublished results of Suh, Frederickson, and Thompson). Stimulation was 0.1 msec 500 uA pulses at 100 Hz for 5 seconds. Images were acquired in an Olympus inverted microscope with a 4X objective; the results represent a small area of the field near the stimulating electrode.

The same approach may be used with *in vivo* dialysis collection approaches.

Future prospects: An expressable Zn indicator?

The issues associated with introducing the carbonic anhydrase molecule into the cell are by now widely appreciated, and several expedients have been described for doing this. Among the potential means are injection (Suh *et al.*, unpublished results) electroporation, and introduction of labeled particles (PEBBLES) by gas gun (Clark *et al.* 1999). One potential approach to calcium ion sensing described by Tsien's group is to express the transducer molecule inside the cell by recombinant DNA techniques, using variants of the Green Fluorescent Protein (GFP) from *Aequorea* (Miyawaki *et al.* 1997) as covalently attached label(s). The issue is how to get the binding of zinc to a carbonic anhydrase molecule to perturb (hopefully increase) the intensity of a GFP attached to the CA molecule. This prospect is daunting inasmuch as the fluorophore moiety in GFP is well shielded from outside influences, and typically has a very good quantum yield; indeed, in this context it might be said that GFP suffers from the defects of its virtues. A GFP sufficiently modified to permit zinc binding to perturb its fluorescence might also no longer be very fluorescent. However, the value of this approach, particularly for *in vitro* studies, suggests that it should be pursued if possible. Two approaches which appear promising have been recently described. Pearce and her colleagues (Pearce *et al.* 2000) described a fusion protein consisting of a metallothionein sandwiched between GFP variants capable of energy transfer. While the authors did not report a metal titration, treatment with EDTA to remove metal from the metallothionein resulted in modest changes in energy transfer, suggesting a conformational change had occurred. Jensen *et al.*, 2001 engineered a multidentate zinc binding site with ligands on two different tethered GFP variants capable of energy transfer. In the presence of zinc the variants are brought closer together by mutually binding a zinc ion, with concomitant energy transfer. This approach also succeeded, but the zinc sensitivity was modest at just under millimolar. Both these efforts underscore the power of Tsien's approach, but clearly more work is needed.

References

Alberts IL, Nadassy K. 1998 Analysis of zinc binding sites in protein crystal structures. *Protein Sci* **7**, 1700–1716.

Belli SL, Zirino A. 1993 Behavior and calibration of the copper(II) ion-selective electrode in high chloride media and marine waters. *Anal Chem* **65**, 2583–2589.

Benters A, Flogel U, Schafer T, Leibfritz D, Hechtenberg S, Beyersmann D. 1997 Study of the interactions of cadmium and zinc ions with cellular calcium homeostasis using $_{19}$F-NMR spectroscopy. *Biochem J* **322**, 793–799.

Chen RF, Kernohan J. 1967 Combination of bovine carbonic anhydrase with a fluorescent sulfonamide. *J Biol Chem* **242**, 5813–5823.

Christianson DW. 1991 Structural biology of zinc. *Adv Prot Chem* **42**, 281–355.

Christianson DW, Alexander RS. 1989 Carboxylate histidine zinc interactions in protein – structure and function. *J Am Chem Soc* **111**, 6412–6419.

Christianson DW, Fierke CA. 1996 Carbonic anhydrase – Evolution of the zinc binding site by nature and by design. *Acc Chem Res* **29**, 331–339.

Clark HA, Hoyer M, Philbert MA, Kopelman R. 1999 Optical nanosensors for chemical analysis inside single living cells. 1. Fabrication, characterization, and methods for intracellular delivery of PEBBLE sensors. *Anal Chem* **71**, 4831–4836.

Cox JD, Hunt JA, Compher KM, Fierke CA, Christianson DW. 2000 Structural influence of hydrophobic core residues on metal binding and specificity in carbonic anhydrase II. *Biochemistry* **39**, 13687–13694.

Denny MF, Atchison WD. 1994 Methylmercury-induced elevations in intrasynaptosomal zinc concentrations: an $_{19}$F-NMR study. *J Neurochem* **63**, 383–386.

DiTusa CA, McCall KA, Christensen T, Mahapatro M, Fierke CA, Toone EJ. 2001 Thermodynamics of metal ion binding. II. Metal ion binding by carbonic anhydrase variants. *Biochemistry*, **40**, 5345–5351.

Dix JA, Verkman AS. 1990 Mapping of fluorescence anisotropy in living cells by ratio imaging: Application to cytoplasmic viscosity. *Biophys J* **57**, 231–240.

Eigen M, Hammes GG. 1963 Elementary steps in enzyme reactions as studied by relaxation spectrometry. *Adv Enzymol Relat Areas Mol Biol* **25**, 1–38.

Elbaum D, Nair SK, Patchan MW, Thompson RB, Christianson DW. 1996 Structure-based design of a sulfonamide probe for fluorescence anisotropy detection of zinc with a carbonic anhydrase-based biosensor. *J Am Chem Soc* **118**, 8381–8387.

Eriksson AE, Jones TA. 1988 Refined structure of human carbonic anhydrase II at 2.0 A resolution. *Proteins* **4**, 274–282.

Fernandez-Gutierrez A, Munoz de la Pena A. 1985 Determinations of inorganic substances by luminescence methods. In: Schulman S.G. ed. *Molecular Luminescence Spectroscopy, Part I: Methods and Applications;* New York: Wiley-Interscience, 371–546.

Frederickson CJ, Suh SW, Silva D, Frederickson CJ, Thompson RB. 2000 Importance of zinc in the central nervous system: the zinc-containing neuron. *J Nutr (Suppl.)* **130**, 1471S–1483S.

Fushimi K, Dix JA, Verkman AS. 1990 Cell membrane fluidity in the intact kidney proximal tubule measured by orientation-independent fluorescence anisotropy imaging. *Biophys J* **57**, 241–254.

Glusker JP. 1991 Structural aspects of metal liganding. *Adv Prot Chem* **42**, 1–76.

Grynkiewicz G, Poenie M, Tsien RY. 1985 A new generation of calcium indicators with greatly improved fluorescence properties. *J Biol Chem* **260**, 3440–3450.

Hakansson K, Carlsson M, Svensson LA, Liljas A. 1992 Structure of native and apo carbonic anhydrase II and structure of some of its anion-ligand complexes. *J Mol Biol* **227**, 1192–1204.

Hakansson K, Wehnert A, Liljas A. 1994 X-ray analysis of metal-substituted human carbonic anhydrase II derivatives. *Acta Crys* **D50**, 93–100.

Haugland RP. 1996 *Handbook of Fluorescent Probes and Research Chemicals*. Oregon: Molecular Probes, Inc., Eugene.

Henkens RW, Sturtevant JM. 1968 The kinetics of the binding of Zn(II) by apocarbonic anhydrase. *J Am Chem Soc* **90**, 2669–2676.

Hirano T, Kikuchi K, Urano Y, Higuchi T, Nagano T. 2000 Highly zinc-selective fluorescent sensor molecules suitable for biological applications. *J Am Chem Soc* **122**, 12399–12400.

Huang C-C, Lesburg CA, Kiefer LL, Fierke CA, Christianson DW. 1996 Reversal of the hydrogen bond to zinc ligand histidine-119 dramatically diminishes catalysis and enhances metal equilibration kinetics in carbonic anhydrase II. *Biochemistry 35*, 3439–3446.

Hunt JA, Ahmed M, Fierke CA. 1999 Metal binding specificity in carbonic anhydrase is influenced by conserved hydrophobic amino acids. *Biochemistry* **38**, 9054–9060.

Hunt JA, Fierke CA. 1997 Selection of carbonic anhydrase variants displayed on phage: aromatic residues in zinc binding site enhance metal affinity and equilibration kinetics. *J Biol Chem* **272**, 20364–20372.

Ippolito JA, Baird TT, McGee SA, Christianson DW, Fierke CA. 1995a Structure-assisted redesign of a protein-zinc binding site with femtomolar affinity. *Proc Natl Acad Sci USA* **92**, 5017–5021.

Ippolito JA, Christianson DW. 1993 Structure of a His^3Cys zinc binding site in human carbonic anhydrase II. *Biochemistry* **32**, 9901–9905.

Ippolito JA, Christianson DW. 1994 Structural consequences of redesigning a protein-zinc binding site. *Biochemistry* **33**, 15241–15249.

Ippolito JA, Nair SK, Fierke CA, Christianson DW. 1995b Structure of His94Asp carbonic anhydrase II in a new crystalline form reveals a partially occupied zinc binding site. *Prot Engin* **8**, 975–980.

Iverson TM, Alber BE, Kisker C, Ferry JG, Rees DC. 2000 A closer look at gamma-class carbonic anhydrases: high resolution crystallographic studies of the carbonic anhydrase from *Methanosarcina thermophila*. *Biochemistry* **39**, 9222–9231.

Jensen KK, Martini L, Schwartz TW. 2001 Enhanced fluorescence resonance energy transfer between spectral variants of green fluorescent protein through zinc-site engineering. *Biochemistry* **40**, 938–945.

Kiefer LL, Fierke CA. 1994 Functional characterization of human carbonic anhydrase II variants with altered zinc binding sites. *Biochemistry* **33**, 15233–15240.

Kiefer LL, Ippolito JA, Fierke CA, Christianson DW. 1993a Redesigning the zinc binding site of human carbonic anhydrase II: Structure of a His^2Asp-Zn_{2+} metal coordination polyhedron. *J Am Chem Soc* **115**, 12581–12582.

Kiefer LL, Krebs JF, Fierke CA. 1993b Engineering a cysteine residue into the zinc binding site of carbonic anhydrase II. *Biochemistry* **32**, 9896–9900.

Kiefer LL, Paterno SA, Fierke CA. 1995 Hydrogen bond network in the metal binding site of carbonic anhydrase enhances zinc affinity and catalytic efficiency. *J Am Chem Soc* **117**, 6831–6837.

Kimber MS, Pai EF. 2000 The active site architecture of *Pisum sativum* beta-carbonic anhydrase is a mirror image of that of alpha-carbonic anhydrases. *EMBO J* **19**, 1407–1418.

Kuhn MA, Hoyland B, Carter S, Zhang C, Haugland RP. 1995 Fluorescent ion indicators for detecting heavy metals. *SPIE Conference on Adv Fluor Sens Tech II* (*San Jose, California*), Vol. 2388, 238–244.

Lesburg CA, Christianson DW. 1995 X-ray crystallographic studies of engineered hydrogen bond networks in a protein-zinc binding site. *J Am Chem Soc* **117**, 6838–6844.

Lesburg CA, Huang C-C, Christianson DW, Fierke CA. 1997 Histidine to carboxamide ligand substitutions in the zinc binding site of carbonic anhydrase II alter metal coordination geometry but retain catalytic activity. *Biochemistry* **36**, 15780–15791.

Levy R, Guignon EF, Cobane S, St. Louis E, Fernandez S. 1997 Compact, rugged, and inexpensive frequency domain fluorometer. *SPIE Conference on Advances in Fluorescence Sensing Technology III*, San Jose, CA vol. 2980, 81–89.

Lindskog S, Henderson LE, Kannan KK, Liljas A, Nyman PO, Strandberg B. 1971 Carbonic anhydrase. In: Boyer PD, ed. *The Enzymes*. New York: Academic Press: 587–665.

Lindskog S, Nyman PO. 1964 Metal-binding properties of human erythrocyte carbonic anhydrases. *Biochim Biophys Acta* **85**, 462–474.

Lippitsch ME, Pusterhofer J, Leiner MJP, Wolfbeis OS. 1988 Fiber-optic oxygen sensor with the fluorescence decay time as the information carrier. *Anal Chim Acta* **205**, 1–6.

Maren TH. 1977 Use of inhibitors in physiological studies of carbonic anhydrase. *Am J Physiol* **232**, F291–F297.

McCall KA, Fierke CA. 2000 Colorimetric and fluorimetric assays to quantitate micromolar concentrations of transition metals. *Anal Biochemistry* **284**, 307–315.

Mitsuhashi S, Mizushima T, Yamashita E, Yamamoto M, Kumasaka T, Moriyama H, Ueki T, Miyachi S, Tsukihara T. 2000 X-ray structure of beta carbonic anhydrase from the red alga, *Porphyridium purpureum*, reveals a novel catalytic site for CO_2 hydration. *J Biol Chem* **275**, 5521–5526.

Miyawaki A, Llopis J, Heim R, McCaffery JM, Adams JA, Ikura M, Tsien RY. 1997 Fluorescent indicators for Ca_{2+} based on green fluorescent proteins and calmodulin. *Nature* **388**, 882–887.

Pearce LL, Gandley RE, Han W, Wasserloos K, Stitt M, Kanai AJ, McLaughlin MK, Pitt BR, Levitan ES. 2000 Role of metallothionein in nitric oxide signaling as revealed by a green fluorescent fusion protein. *Proc Natl Acad Sci USA* **97**, 477–482.

Pearson RG. 1966 Acids and bases. *Science* **151**, 172–177.

Rae TD, Schmidt PJ, Pufahl RA, Culotta VC, O'Halloran TV. 1999 Undetectable intracellular free copper: the requirement of a copper chaperone for superoxide dismutase. *Science* **284**, 805–808.

Roe RR, Pang YP. 1999 Zinc's exclusive tetrahedral coordination governed by its electronic structure. *J Mol Model* **5**, 134–140.

Rulisek L, Vondrasek J. 1998 Coordination geometries of selected transition metal ions (Co_{2+}, Ni_{2+}, Cu_{2+}, Zn_{2+}, Cd2+, and Hg_{2+}) in metalloproteins. *J Inorg Biochem* **71**, 115–127.

Simons TJB. 1993 Measurement of free zinc ion concentration with the fluorescent probe mag-fura-2 (furaptra). *J Biochem Biophys Meth* **27**, 25–37.

Szmacinski H, Lakowicz JR. 1993 Optical measurements of pH using fluorescence lifetimes and phase-modulation fluorometry. *Anal Chem* **65**, 1668–1674.

Thompson RB. 1991 Fluorescence-based fiber optic sensors. In: Lakowicz JR, ed. *Topics in Fluorescence Spectroscopy. Vol. 2: Principles*. New York: Plenum Press: 345–365.

Thompson RB. 1993 Fiber optic ion sensors based on phase fluorescence lifetime measurements. *SPIE Conference on Advances in Fluorescence Sensing Technology*, Los Angeles, CA, vol. 1885, 290–299.

Thompson RB, Frisoli JK, Lakowicz JR. 1992 Phase fluorometry using a continuously modulated laser diode. *Anal Chem* **64**, 2075–2078.

Thompson RB, Ge Z, Patchan MW, Fierke CA. 1996a Performance enhancement of fluorescence energy transfer-based biosensors by site-directed mutagenesis of the transducer. *J Biomed Optics* **1**, 131–137.

Thompson RB, Ge Z, Patchan MW, Huang C-C, Fierke CA. 1996b Fiber optic biosensor for Co(II) and Cu(II) based on fluorescence energy transfer with an enzyme transducer. *Biosensors Bioelectron* **11**, 557–564.

Thompson RB, Jones ER. 1993 Enzyme-based fiber optic zinc biosensor. *Anal Chem* **65**, 730–734.

Thompson RB, Whetsell WO Jr., Maliwal BP, Fierke CA, Frederickson CJ. 2000a Fluorescence microscopy of stimulated Zn(II) release from organotypic cultures of mammalian hippocampus using a carbonic anhydrase-based biosensor system. *J Neurosci Meth* **96**, 35–45.

Thompson RB, Maliwal BP, Feliccia VL, Fierke CA, McCall K. 1998a Determination of picomolar concentrations of metal ions using fluorescence anisotropy: biosensing with a 'reagentless' enzyme transducer. *Anal Chem* **70**, 4717–4723.

Thompson RB, Maliwal BP, Fierke CA. 1998b Expanded dynamic range of free zinc ion determination by fluorescence anisotropy. *Anal Chem* **70**, 1749–1754.

Thompson RB, Maliwal BP, Fierke CA. 1999 Selectivity and sensitivity of fluorescence lifetime-based metal ion biosensing using a carbonic anhydrase transducer. *Anal Biochem* **267**, 185–195.

Thompson RB, Maliwal BP, Zeng HH. 2000b Zinc biosensing with multiphoton excitation using carbonic anhydrase and improved fluorophores. *J Biomed Optics* **5**, 17–22.

Thompson RB, Patchan MW. 1995a Fluorescence lifetime-based biosensing of zinc: origin of the broad dynamic range. *J Fluoresc* **5**, 123–130.

Thompson RB, Patchan MW. 1995b Lifetime-based fluorescence energy transfer biosensing of zinc. *Anal Biochem* **227**, 123–128.

Thompson RB, Walt DR. 1994 Emerging strategies for molecular biosensors. *Naval Res Rev* **46**, 19–29.

Thompson RB, Zeng HH, Loetz M, Fierke C. 2000 Issues in enzyme-based metal ion biosensing in complex media. *In-vitro Diagnostic Instrumentation* (*San Jose, CA*), vol. 3913, 120-127.

Weber G. 1956 Photoelectric method for the measurement of polarization of fluorescence of solutions. *J Opt Soc Am* **46**, 962.

White CE, Argauer RJ. 1970 *Fluorescence Analysis: A Practical Approach*. New York: Marcel Dekker, Inc.

Yamashita MM, Wesson L. 1990 Where metal ions bind in proteins. *Proc Natl Acad Sci USA* **87**, 5648–5652.